Determination of the Neutron Spin Structure Function

P. L. Anthony,[6] R. G. Arnold,[1] H. R. Band,[13] H. Borel,[4] P. E. Bosted,[1] V. Breton,[2] G. D. Cates,[9] T. E. Chupp,[7] F. S. Dietrich,[6] J. Dunne,[1] R. Erbacher,[11] J. Fellbaum,[1] H. Fonvieille,[2] R. Gearhart,[10] R. Holmes,[12] E. W. Hughes,[10] J. R. Johnson,[13] D. Kawall,[11] C. Keppel,[1] S. E. Kuhn,[8] R. M. Lombard-Nelsen,[4] J. Marroncle,[4] T. Maruyama,[10] W. Meyer,[10] Z.-E. Meziani,[11] H. Middleton,[9] J. Morgenstern,[4] N. R. Newbury,[9] G. G. Petratos,[10] R. Pitthan,[10] R. Prepost,[13] Y. Roblin,[2] S. E. Rock,[1] S. H. Rokni,[10] G. Shapiro,[3] T. Smith,[7] P. A. Souder,[12] M. Spengos,[1] F. Staley,[4] L. M. Stuart,[10] Z. M. Szalata,[1] Y. Terrien,[4] A. K. Thompson,[5] J. L. White,[1] M. Woods,[10] J. Xu,[12] C. C. Young,[10] and G. Zapalac[13]

(E142 Collaboration)

[1]*American University, Washington, D.C. 20016*
[2]*Laboratoire de Physique Corpusculaire, Institut Nationale de Physique Nucléaire et de Physique des Particules/Centre Nationale de la Recherche Scientifique, Université Blaise Pascal, F-63170 Aubière Cedex, France*
[3]*University of California and Lawrence Berkeley Laboratory, Berkeley, California 94720*
[4]*Département de Physique Nucléaire, Centre d' Etudes Nucléaire de Saclay, F-91191 Gif-sur-Yvette Cedex, France*
[5]*Harvard University, Cambridge, Massachusetts 02138*
[6]*Lawrence Livermore National Laboratory, Livermore, California 94550*
[7]*University of Michigan, Ann Arbor, Michigan 48109*
[8]*Old Dominion University, Norfolk, Virginia 23529*
[9]*Princeton University, Princeton, New Jersey 08544*
[10]*Stanford Linear Accelerator Center, Stanford, California 94309*
[11]*Stanford University, Stanford, California 94305*
[12]*Syracuse University, Syracuse, New York 13210*
[13]*University of Wisconsin, Madison, Wisconsin 53706*

(Received 1 April 1993)

The spin structure function of the neutron g_1^n has been determined over the range $0.03 < x < 0.6$ at an average Q^2 of 2 $(\mathrm{GeV}/c)^2$ by measuring the asymmetry in deep inelastic scattering of polarized electrons from a polarized ^{3}He target at energies between 19 and 26 GeV. The integral of the neutron spin structure function is found to be $\int_0^1 g_1^n(x)dx = -0.022 \pm 0.011$. Earlier reported proton results together with the Bjorken sum rule predict $\int_0^1 g_1^n(x)dx = -0.059 \pm 0.019$.

PACS numbers: 13.60.Hb, 13.88.+e, 14.20.Dh, 25.30.Fj

For the past twenty years, results from deep inelastic scattering of polarized electrons and muons by polarized protons have been used to study the internal spin structure of the nucleon [1–3]. These experiments found large asymmetries over a large kinematic range as predicted by the quark-parton model (QPM). However, when interpreted by theoretical sum rules as described below, the data indicate that only a small fraction of the proton spin is carried by the quarks and that the strange sea polarization is large and negative. A complete understanding of nucleon spin structure requires information from neutron as well as more precise proton measurements. In this Letter we report new measurements of the neutron spin structure function g_1^n using longitudinally polarized electron scattering from a polarized ^{3}He target in End Station A at SLAC.

The spin structure functions G_1 and G_2 can be determined experimentally by measuring the difference in cross sections of polarized electrons on polarized nucleons between states where the spins are parallel and antiparallel [4,5],

$$\frac{d^2\sigma^{\uparrow\downarrow}}{dQ^2dv} - \frac{d^2\sigma^{\uparrow\uparrow}}{dQ^2dv} = \frac{4\pi\alpha^2}{Q^2E^2}[M(E+E'\cos\theta)G_1(Q^2,v) - Q^2G_2(Q^2,v)]. \quad (1)$$

Here M is the mass of the nucleon, v is the electron energy loss, $q^2 = -Q^2$ is the square of the four-momentum of the virtual photon, α is the fine structure constant, E' is the scattered electron energy, E is the incident electron energy, θ is the electron scattering angle, and $d^2\sigma^{\uparrow\uparrow}$ ($d^2\sigma^{\uparrow\downarrow}$) is the differential scattering cross section for longitudinal target spins parallel (antiparallel) to the incident electron spins. A corresponding relationship exists for scattering of longitudinally polarized electrons off a transversely polarized target [5]. In the scaling limit (v and Q^2 large), these structure functions are predicted to depend only on $x = Q^2/2Mv$ yielding $M^2vG_1(v,Q^2) \to g_1(x)$ and $Mv^2G_2(v,Q^2) \to g_2(x)$.

Bjorken [6] developed a sum rule relating the integrals over the proton and neutron spin structure functions to the weak coupling constants g_A and g_V found in nucleon β decay:

$$\int_0^1 [g_1^p(x) - g_1^n(x)]dx = \frac{1}{6}\frac{g_A}{g_V}[1 - \alpha_s(Q^2)/\pi], \quad (2)$$

where $\alpha_s(Q^2)$ is the QCD coupling constant [7,8] and $g_A/g_V = 1.257 \pm 0.003$ [9]. The sum rule, first derived from current algebra, is a rigorous prediction of QCD. Ellis and Jaffe [10] have derived similar sum rules for the proton and neutron based on SU(3) symmetry and the

0031-9007/93/71(7)/959(4)$06.00

assumption that the strange sea is unpolarized:

$$\int_0^1 g_1^{p(n)}(x)dx = \tfrac{1}{18}[9(6)F-1(4)D][1-\alpha_s(Q^2)/\pi]. \quad (3)$$

The constants F and D are SU(3) invariant matrix elements of the axial vector current where for neutron beta decay, $F+D=g_A/g_V$ [11]. The integral over the spin structure functions has a simple interpretation in the QPM:

$$\int_0^1 g_1^{p(n)}(x)dx = \tfrac{1}{2}[\tfrac{4}{9}\Delta u(d)+\tfrac{1}{9}\Delta d(u)+\tfrac{1}{9}\Delta s][1-\alpha_s(Q^2)/\pi], \quad (4)$$

where Δu, Δd, and Δs represent the integral over the quark momentum distributions of the up, down, and strange quarks of the proton defined by

$$\Delta q = \int_0^1 [q^{\uparrow}(x)-q^{\downarrow}(x)]dx,$$

where $q^{\uparrow}(x)$ $[q^{\downarrow}(x)]$ are the quark plus antiquark momentum distributions for quark and antiquark spins parallel [antiparallel] to the nucleon spin. From SU(3) symmetry, the integral over the quark momentum distributions can be related to F and D via $\Delta d-\Delta s=F-D$. In the QPM, the Bjorken sum rule reduces to $\Delta u-\Delta d=F+D$. The European Muon Collaboration (EMC), which provided the first data for $x<0.1$, has reported a value

$$\int_0^1 g_1^p(x)dx = 0.126\pm0.010(\text{stat})\pm0.015(\text{syst})$$

for the proton integral [3], which is smaller than the value 0.175 ± 0.018 [11] from Eq. (3). In the QPM this result can be interpreted to mean that the total quark contribution to the proton spin is small ($\Delta u+\Delta d+\Delta s=0.13\pm0.19$), whereas the strange sea contribution is large and negative ($\Delta s=-0.16\pm0.08$).

The experimental quantities used to determine the spin structure functions are the two asymmetries:

$$A^{\parallel}=\frac{d\sigma^{\uparrow\downarrow}-d\sigma^{\uparrow\uparrow}}{d\sigma^{\uparrow\downarrow}+d\sigma^{\uparrow\uparrow}}, \quad A^{\perp}=\frac{d\sigma^{\uparrow\leftarrow}-d\sigma^{\uparrow\leftarrow}}{d\sigma^{\downarrow\leftarrow}+d\sigma^{\uparrow\leftarrow}}. \quad (5)$$

Here $d\sigma^{\downarrow\leftarrow}$ $(d\sigma^{\uparrow\leftarrow})$ is the scattering cross section for beam spin antiparallel (parallel) to the beam momentum and target spin direction transverse to the beam momentum and towards the direction of the scattered electron, and $d\sigma^{\uparrow\downarrow}$ $(d\sigma^{\uparrow\uparrow})$ is defined in Eq. (1). The experimental asymmetries $A^{\parallel}$ and $A^{\perp}$ are related to the virtual photon-nucleon longitudinal and transverse symmetries, A_1 and A_2, respectively, via $A^{\parallel}=D(A_1+\eta A_2)$ and $A^{\perp}=d(A_2-\zeta A_1)$, where $D=(1-E'\epsilon/E)/(1+\epsilon R)$, $\eta=\epsilon\sqrt{Q^2}/(E-E'\epsilon)$, $d=D\sqrt{2\epsilon/(1+\epsilon)}$, $\zeta=\eta(1+\epsilon)/2\epsilon$, and $1/\epsilon=1+2[1+(\nu^2/Q^2)]\tan^2(\theta/2)$. Here R is the ratio of longitudinal to transverse virtual photoabsorption cross sections. The neutron spin structure function is extracted via

$$g_1^n=[A_1^nF_1^n+A_2^nF_1^n(2Mx/\nu)^{1/2}]/(1+2Mx/\nu),$$

where F_1^n is the spin averaged structure function of the neutron.

The SLAC polarized electron beam was created by photoemission from an AlGaAs photocathode [12] illuminated by a flash lamp pumped dye laser [13]. The polarized source delivered between 0.5 and 2.0×10^{11} electrons per pulse at 120 Hz. The pulse length varied from 0.8 to 1.4 μsec. The electron helicity was reversed randomly on a pulse-to-pulse basis by reversing the source laser circular polarization. Frequent helicity reversal is important because it avoids the introduction of false asymmetries from drifts in the operation of the beam, target, or spectrometers. The beam polarization was measured by a single-arm Møller polarimeter and was observed to be very stable and constant over the full run with an average value of $(38.8\pm1.6)\%$. The largest uncertainty arises from the measurement of the magnetization of the Møller target foils.

The ^{3}He nuclei in the gas target were polarized through spin-exchange collisions with optically pumped rubidium vapor. A two-chambered design was used [14] (Fig. 1). The target chamber had a length of 30 cm with 0.012 cm thick end windows and operated with a ^{3}He density of 2.3×10^{20} atoms/cm^3 (8.6 atm at 0 °C). A small amount of nitrogen ($\sim1.9\times10^{18}$ atoms/cm^3) increased the optical pumping efficiency. Five high-power laser systems produced 20 W cw of near infrared laser light for optical pumping. The ^{3}He polarization was measured with NMR techniques with an uncertainty of $\Delta P_t/P_t$ of 7%. The largest contribution came from the uncertainty in the NMR calibration measurements of the thermal equilibrium polarization of protons in water. P_t varied slowly between 30% and 40% during the experiment; its direction was reversed frequently to cancel systematic false asymmetries.

Data were collected at three different beam energies, 19.4, 22.7, and 25.5 GeV covering a range in x from 0.03 to 0.6 with Q^2 greater than 1 $(\text{GeV}/c)^2$. The total event sample amounted to $\sim4\times10^8$ electrons collected in two single-arm magnetic spectrometers [15], at horizontal scattering angles of 4.5° and 7° (Fig. 2). The detectors in each spectrometer consisted of two N_2 threshold Čerenkov counters, six planes of hodoscopes, and a 24 radiation length shower counter composed of 200 lead glass blocks. Each spectrometer accepted charged particles with momenta greater than ~6 GeV/c. The momentum resolution (rms) from hodoscope tracking was $\Delta E'/E'\sim3\%$ on average, and the shower energy resolution was typically $15\%/\sqrt{E'\,(\text{GeV})}$.

The experimental asymmetry $A^{\parallel}$ is derived from the measured raw counting rate asymmetry $\Delta=(N^{\uparrow\downarrow}-N^{\uparrow\uparrow})/(N^{\uparrow\downarrow}+N^{\uparrow\uparrow})=A^{\parallel}P_tP_bf$ where $N^{\uparrow\uparrow}$ and $N^{\uparrow\downarrow}$ represent the number of scattered electrons per incident beam electron in the spectrometer when the beam and target spins are parallel and antiparallel, respectively. Here, P_t and P_b are the target and beam polarizations. The dilution factor f is the fraction of events originating

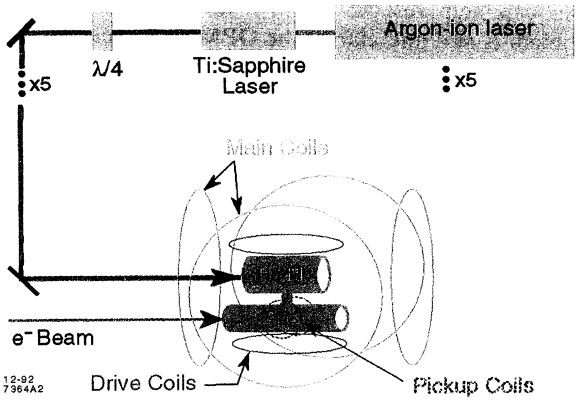

FIG. 1. Schematic layout of the polarized ^{3}He target. Five sets of lasers optically pump rubidium vapor in the top chamber for polarization of ^{3}He nuclei. Incident electrons scatter off the nuclei in the bottom chamber. Two sets of Helmholtz coils hold the target spins in the longitudinal or transverse direction. Drive and pickup coils are used to measure polarization.

from polarized neutrons in the target ($f \sim 0.11 \pm 0.02$ and varies slowly with x). All counting rates were corrected for deadtime and normalized to the total incident charge as measured by two independent toroidal charge monitors. Beam charge differences between parallel and antiparallel polarized electrons were measured to be on the order of 1 part in 10^4.

Electrons were identified by a coincidence of the two Čerenkov counters and a large pulse height in the shower counter. Electron energy and position in the shower counter determined the x and Q^2 of the event. Hodoscope tracking was used for systematic studies and for the absolute energy calibration of the lead glass. The electron background from charge-symmetric processes was determined to be $\sim 5\%$ of the electron sample at low x by measuring the positron rate in runs with the spectrometer magnet polarity reversed. The background from misidentified pions was studied using a comparison of momentum from tracking to shower energy deposition and contributed about 2% to the electron sample at low x. Contaminations in the high x bins were negligible. Glass cell runs with variable pressures of ^{3}He were used to study the dilution factor by separating contributions from scattering off ^{3}He versus glass. The largest systematic

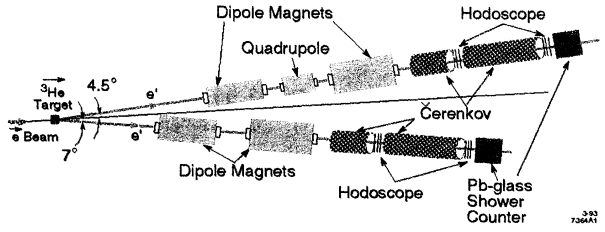

FIG. 2. Layout of the experimental setup. Two independent single-arm spectrometers are shown.

uncertainty in this experiment comes from the determination of the dilution factor to $\pm 15\%$ of its value. False asymmetries were found to be consistent with zero by comparing data with target spins in opposite directions.

Internal spin-dependent radiative corrections were calculated using the complete Kukhto and Shumeiko formulas [16] (exact integration, no peaking approximation). External radiative corrections followed Mo and Tsai [17], but were small because the target was thin ($\sim 0.3\%$ radiation length). The total corrections amounted to a relative change in the asymmetry ranging from $(30 \pm 15)\%$ at low x to $(5 \pm 2)\%$ at high x. The uncertainty from the radiative corrections takes into account variations due to the model dependence on the corrections.

A polarized ^{3}He nucleus is regarded as a good model of a polarized neutron for deep inelastic scattering [18,19]. The ^{3}He wave function is primarily in an S-state in which the two protons pair with opposite spins due to the Pauli exclusion principle, leaving the neutron spin as the dominant contribution to spin-dependent scattering. A small correction from the polarization of the two protons in ^{3}He ($\sim -2.7\%$ per proton) and a correction for the polarization of the neutron in ^{3}He ($\sim 87\%$) were applied in order to extract the neutron asymmetry from the measured ^{3}He asymmetry [20,21]. For the proton correction, the asymmetry results from EMC were taken [3]. No other corrections were made because of the fact that the polarized neutron is embedded in the ^{3}He nucleus.

The physics asymmetry A_1^n vs x is presented in Fig. 3. Since no significant Q^2 dependence of the measurements was observed, the data at different energies for fixed x bins are averaged over Q^2. A clear trend of negative asymmetries is evident. Measurements of the transverse neutron asymmetry A_2^n were found to be consistent with zero with statistical uncertainties of typically ± 0.25. The lower part of Fig. 3 shows the neutron spin structure function extracted from the measured asymmetries, using the results from a global fit to SLAC structure function data [22].

The integral of the spin structure function over the measured range of x is

$$\int_{0.03}^{0.6} g_1^n(x)dx = -0.019 \pm 0.007(\text{stat}) \pm 0.006(\text{syst})$$

at an average Q^2 of 2 $(\text{GeV}/c)^2$. Propagating the unpolarized structure function to Q^2 of 2 $(\text{GeV}/c)^2$ for all x bins gives the same result. Extrapolation of the spin structure function outside the measured x range requires models of the neutron spin structure. Assuming perturbative QCD, the asymmetry A_1^n approaches 1 as x approaches 1. Using this constraint and a Regge parametrization ($A_1^n \sim x^{1.2}$) to fit the low x data [23], the neutron integral is extracted over the full x range, $\int_0^1 g_1^n(x)dx = -0.022 \pm 0.011$. The extrapolations to low and high x amounted to additions to the measured integral of -0.006 ± 0.006 and 0.003 ± 0.003, respectively. Combining the integral over the neutron spin structure func-

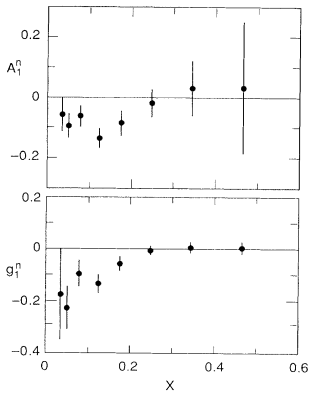

FIG. 3. Results for neutron asymmetries A_1^n and the neutron spin structure function g_1^n as a function of x averaged over Q^2. Statistical and systematic errors are added in quadrature.

tion from this experiment with the proton integral from EMC [3] corrected to Q^2 of 2 $(\mathrm{GeV}/c)^2$ gives the integral $\int_0^1 [g_1^p(x) - g_1^n(x)]dx = 0.146 \pm 0.021$. This is to be compared to a Bjorken sum rule prediction of 0.183 ± 0.007 using $\alpha_s = 0.39 \pm 0.10$ at Q^2 of 2 $(\mathrm{GeV}/c)^2$. Higher order QCD corrections [24] or higher twist effects [25] may account for the apparent discrepancy.

The results from this experiment in conjunction with the weak coupling constants from baryon decay, $F = 0.47 \pm 0.04$ and $D = 0.81 \pm 0.03$ [11], can be used to extract the integral over the quark spin distributions from the QPM using $\alpha_s = 0.385$ at Q^2 of 2 $(\mathrm{GeV}/c)^2$. The results yield $\Delta u = 0.93 \pm 0.06$, $\Delta d = -0.35 \pm 0.04$, and $\Delta s = -0.01 \pm 0.06$. These results imply that the total quark contribution to the nucleon spin $(\Delta u + \Delta d + \Delta s)$ is 0.57 ± 0.11. Thus, the quarks contribute approximately one-half of the nucleon spin, and the strange sea contribution is small. Orbital angular momentum [26] and the spin of the gluons [27] may account for the remaining nucleon spin.

A new measurement on the deuteron by the Spin Muon Collaboration combined with the EMC proton result leads to a neutron integral of $-0.08 \pm 0.04(\mathrm{stat}) \pm 0.04(\mathrm{syst})$ [28]. Within the 6 times larger error, this result is consistent with ours.

We have presented results on the neutron spin structure function and used them to test QCD sum rules. When combined with the proton results from EMC, the results from this experiment differ from the Bjorken sum rule prediction evaluated to first order in α_s by ~ 2 standard deviations. Within present theoretical uncertainties on the corrections to the Bjorken sum rule, the discrepancy is of marginal significance. Our results give a reasonable QPM interpretation and good agreement with the updated value of the Ellis-Jaffe sum rule [11] $\int_0^1 g_1^n(x)dx = -0.021 \pm 0.018$ at a Q^2 of 2 $(\mathrm{GeV}/c)^2$. The striking difference between the EMC QPM interpretation and ours is at the same 2-standard-deviation level as the Bjorken sum rule difference. More precise proton data can help resolve whether the 2-standard-deviation problem is real and clarify the QPM interpretation.

This work was supported by Department of Energy Contracts No. DE-AC03-76SF0900098 (LBL), No. W-2705-Eng-48 (LLNL), No. DE-FG02-90ER40557 (Princeton), No. DE-AC03-76SF00515 (SLAC), No. DE-FG03-88ER40439 (Stanford), No. DE-FG02-84-ER40146 (Syracuse), and No. DE-AC02-76ER00881 (Wisconsin), and National Science Foundation Grants No. 9014406, No. 9114958 (American), No. 8914353, No. 9200621 (Michigan), and the Bundesministerium für Forschung und Technologie (W.M.).

[1] M. J. Alguard *et al.*, Phys. Rev. Lett. **37**, 1258 (1976); **37**, 1261 (1976).
[2] G. Baum *et al.*, Phys. Rev. Lett. **51**, 1135 (1983).
[3] J. Ashman *et al.*, Phys. Lett. B **206**, 364 (1988); Nucl. Phys. **B328**, 1 (1989).
[4] C. E. Carlson and W.-K. Tung, Phys. Rev. D **5**, 721 (1972).
[5] A. J. G. Hey and J. E. Mandula, Phys. Rev. D **5**, 2610 (1972).
[6] J. D. Bjorken, Phys. Rev. **148**, 1467 (1966); Phys. Rev. D **1**, 1376 (1970).
[7] J. Kodaira *et al.*, Phys. Rev. D **20**, 627 (1979).
[8] J. Kodaira *et al.*, Nucl. Phys. **B159**, 99 (1979); **B165**, 129 (1980).
[9] Particle Data Group, Review of Particle Properties, Phys. Rev. D **45**, 1 (1992).
[10] J. Ellis and R. Jaffe, Phys. Rev. D **9**, 1444 (1974).
[11] R. L. Jaffe and A. V. Manohar, Nucl. Phys. **B337**, 509 (1990).
[12] T. Maruyama *et al.*, J. Appl. Phys. **73**, 5189 (1993).
[13] M. Woods *et al.*, Report No. SLAC-PUB-5965, 1992 (unpublished).
[14] T. E. Chupp *et al.*, Phys. Rev. C **45**, 915 (1992); **36**, 2244 (1987).
[15] G. G. Petratos *et al.*, Report No. SLAC-PUB-5678, 1991 (unpublished).
[16] T. V. Kukhto and N. M. Shumeiko, Nucl. Phys. **B219**, 412 (1983).
[17] L. W. Mo and Y. S. Tsai, Rev. Mod. Phys. **41**, 205 (1969).
[18] R. M. Woloshyn, Nucl. Phys. **496A**, 749 (1989).
[19] C. Ciofi degli Atti *et al.*, University of Perugia Report No. DFUPG-75/93 (to be published).
[20] B. Blankleider and R. M. Woloshyn, Phys. Rev. C **29**, 538 (1984).
[21] J. L. Friar *et al.*, Phys. Rev. C **42**, 2310 (1990).
[22] L. W. Whitlow *et al.*, Phys. Lett. B **250**, 193 (1990); **282**, 475 (1992).
[23] A. Schafer, Phys. Lett. B **208**, 175 (1988).
[24] S. A. Larin and J. A. M. Vermaseren, Phys. Lett. B **259**, 345 (1991).
[25] I. I. Balitsky *et al.*, Phys. Lett. B **242**, 245 (1990).
[26] J. Ellis and M. Karliner, Phys. Lett. B **213**, 73 (1988).
[27] G. Altarelli and G. G. Ross, Phys. Lett. B **212**, 391 (1988).
[28] B. Adeva *et al.*, Phys. Lett. B **362**, 553 (1993).

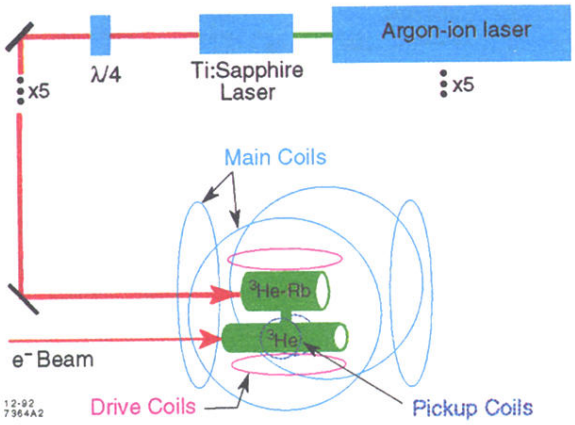

FIG. 1. Schematic layout of the polarized ^{3}He target. Five sets of lasers optically pump rubidium vapor in the top chamber for polarization of ^{3}He nuclei. Incident electrons scatter off the nuclei in the bottom chamber. Two sets of Helmholtz coils hold the target spins in the longitudinal or transverse direction. Drive and pickup coils are used to measure polarization.

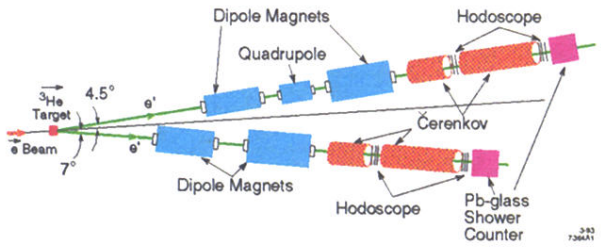

FIG. 2. Layout of the experimental setup. Two independent single-arm spectrometers are shown.